Eur. Phys. J. C (2018) 78:648
https://doi.org/10.1140/epjc/s10052-018-6134-0

THE EUROPEAN PHYSICAL JOURNAL C

CrossMark

Regular Article - Theoretical Physics

Regge trajectories for the mesons consisting of different quarks

Jiao-Kai Chen[a]

School of Physics and Information Science, Shanxi Normal University, Linfen 041004, China

Received: 8 July 2018 / Accepted: 3 August 2018 / Published online: 14 August 2018

Abstract By applying the Bohr–Sommerfeld quantization approach to the quadratic form of the spinless Salpeter-type equation (QSSE), we show that the obtained Regge trajectories for the mesons consisting of unequally massive quarks take the form $M^2 = \beta(c_l l + \pi n_r + c_0)^{2/3} + c_1$, which have the same form as the Regge trajectories for charmonia and bottomonia. Then we apply the obtained Regge trajectories to fit the spectra of the strange mesons, the heavy-light mesons (the D, D_s, B and B_s mesons) and the bottom-charmed mesons. The fitted Regge trajectories are in agreement with the experimental data and the theoretical predictions, which demonstrates that the newly proposed Regge trajectories can be applied universally to the light mesons, the heavy-light mesons and the heavy mesons. By fitting the spectra of the mesons composed of different quarks, the concavity of these Regge trajectories are illustrated, which is of cardinal significance for the potential models.

1 Introduction

The Regge trajectory is one of the effective approaches for studying hadron spectra [1–22]. For one newly proposed Regge trajectories, checking its universality is an important and necessary task. In Ref. [23], the authors applied the rotational states of the string with massive ends including the spin-orbit correction to describe the Regge trajectories for the light, strange, charmed, bottom mesons, and for the $\Delta/\Sigma/\Lambda/\Lambda_c$ baryons. In Ref. [24], the authors used the Regge-like formula $(M - m_Q)^2 = \pi\sigma L$ to analyze all the heavy-light mesons and the baryons which can be assumed consisting of one heavy quark and one light cluster of two light quarks.

In Ref. [25], we proposed one new form of the Regge trajectories,

$$M^2 = \beta(c_l l + \pi n_r + c_0)^{2/3} + c_1, \tag{1}$$

where M is the meson mass, l is the orbital angular momentum, n_r is the radial quantum number. β and c_l are universal parameters. c_0 and c_1 vary with different trajectories. As applying the formula (1) to fit the bottomonia and charmonia, the results are excellent. In the present work, we use the quadratic form of the spinless Salpeter-type equation (QSSE) [26–33] to discuss the Regge trajectories for the mesons consisting of different quarks. We find that the obtained formula can be written in the same form as the Regge trajectories in Eq. (1). The fitted Regge trajectories agree with the experimental data and the theoretical values. By fitting data, we notice that the Regge trajectories for these meson are concave, which is of cardinal significance for the potential models because this property of the Regge trajectories can assist in the choice of the appropriate dynamic equation and potential to describe mesons.

This paper is organized as follows. In Sect. 2, the new form of the Regge trajectories for mesons composed of different quarks is obtained from the QSSE, which has the same form as that for heavy quarkonia. In Sect. 3, the obtained Regge trajectory is applied to fit the spectra of the strange mesons, the heavy-light mesons and the bottom-charmed mesons. In Sect. 4, the universality and concavity of the newly proposed Regge trajectories are discussed. We conclude in Sect. 5.

2 Regge trajectories from the QSSE

In this section, the QSSE is briefly reviewed at first. Then the orbital and radial Regge trajectories for the mesons consisting of unequally massive quarks are obtained from the QSSE by employing the Bohr–Sommerfeld quantization approach [13,34], which have the same form as the Regge trajectories for heavy quarkonia obtained in Ref. [25].

[a] e-mails: chenjk@sxnu.edu.cn;chenjkphy@outlook.com

2.1 QSSE

It is well known that the Bethe–Salpeter equation [35,36] is an appropriate tool to deal with bound states. In Ref. [27], the authors obtained a first principal Bethe–Salpeter equation, and then reduced it to the eigenvalue equation for the square mass operator [26–30] by means of a three dimensional reduction

$$M^2 = M_0^2 + U, \tag{2}$$

where

$$M_0 = \omega_1 + \omega_2 = \sqrt{m_1^2 + \mathbf{p}^2} + \sqrt{m_2^2 + \mathbf{p}^2},$$

$$\langle \mathbf{p}|U|\mathbf{p}'\rangle = \frac{1}{(2\pi)^3}\sqrt{\frac{w_1+w_2}{2w_1w_2}}\,\hat{I}_{ab}^{\text{inst}}(\mathbf{p},\mathbf{p}')\sqrt{\frac{w_1'+w_2'}{2w_1'w_2'}}\sigma_1^a\sigma_2^b. \tag{3}$$

In the above equations, M is the bound state mass, $\mathbf{p}$ the c.m. momentum of quarks, m_1 and m_2 their constituent masses, $\omega_1' = \sqrt{m_1^2+\mathbf{p}'^2}$ and $\omega_2' = \sqrt{m_2^2+\mathbf{p}'^2}$. $\hat{I}_{ab}^{\text{inst}}(\mathbf{p},\mathbf{p}')$ is the instantaneous kernel. Neglecting any reference to the spin degrees of freedom of the involved bound-state constituents, Eq. (2) reduces to the QSSE which is written in configuration space as [29–33]

$$M^2\Psi(\mathbf{r}) = [\omega_1+\omega_2]^2\,\Psi(\mathbf{r}) + \mathcal{U}\Psi(\mathbf{r}), \tag{4}$$

where ω_i is the square-root operator of the relativistic kinetic energy of constituent

$$\omega_i = \sqrt{m_i^2 - \Delta}. \tag{5}$$

Δ is the Laplacian. Let $m_1 \geq m_2$, there is the inequality for M_0^2

$$4(m_2^2+\mathbf{p}^2) \leq M_0^2 \leq 4(m_1^2+\mathbf{p}^2). \tag{6}$$

In case of $|\mathbf{p}| \gg m_1, m_2$, there is

$$M_0^2 \approx 4\mathbf{p}^2 + 2(m_1^2+m_2^2).$$

In case of $|\mathbf{p}| \ll m_1, m_2$, there is

$$M_0^2 \approx \left(2 + \frac{m_1}{m_2} + \frac{m_2}{m_1}\right)\mathbf{p}^2 + (m_1+m_2)^2.$$

For simplicity, we assume that $\mathcal{U}$ takes the following form

$$\mathcal{U} = -\frac{A}{r} + Br, \tag{7}$$

which is a variant of the well-known Cornell potential [37]. A and B vary with the discussed mesons. For example, $A = 2(m_b+m_c)\alpha$ and $B = 2(m_b+m_c)\sigma$ for the bottom-charmed mesons, where m_c and m_b are the charm quark mass and the bottom quark mass, respectively. $\alpha = \alpha_s 4/3$, α_s is the strong coupling constant of the color Coulomb interaction. σ is the string tension.

2.2 Regge trajectories for the mesons composed of different quarks

Due to the $\omega_1\omega_2$ term, the Regge trajectories can not be obtained directly from Eq. (4). Using Eqs. (4), (6) and (7), we propose two auxiliary equations

$$M_i^2\Psi(\mathbf{r}) = 4(m_i^2+\mathbf{p}^2)\Psi(\mathbf{r}) + \left(-\frac{A}{r} + Br\right)\Psi(\mathbf{r}), \quad i = 1, 2, \tag{8}$$

where

$$\mathbf{p}^2 = p_r^2 + \frac{p_\phi^2}{r^2}. \tag{9}$$

Following Refs. [13,25] to employ the Bohr–Sommerfeld quantization approach [34], the orbital Regge trajectories and the radial Regge trajectories can be easily obtained from Eqs. (8),

$$M_i^2 \sim \beta_l l^{2/3}, \quad \beta_l = 3B^{2/3},$$
$$M_i^2 \sim \beta_{n_r} n_r^{2/3}, \quad \beta_{n_r} = (3\pi B)^{2/3}. \tag{10}$$

In case of the power-law potential $V(r) = Br^a$ $(a > 0)$, the orbital Regge trajectories for large l are

$$M_i^2 \sim \beta_l(a) l^{2a/(a+2)} \quad (l \gg n), \tag{11}$$

where $\beta_l(a)$ reads

$$\beta_l(a) = 2^{2a/(a+2)}B^{2/(a+2)}\left(1+\frac{a}{2}\right)\left(\frac{2}{a}\right)^{a/(a+2)}. \tag{12}$$

The radial Regge trajectories are

$$M^2 \sim \beta_{n_r}(a) n_r^{2a/(a+2)} \quad (n_r \gg l). \tag{13}$$

The Regge slope is

$$\beta_{n_r}(a) = 2^{2a/(a+2)}B^{2/(a+2)}\left[\frac{a\pi}{B(1/a, 3/2)}\right]^{2a/(a+2)}, \tag{14}$$

where $B(x, y)$ is the beta function [38].

Using Eqs. (4), (6), (8) and (10), we assume that for Eq. (4) with the potential (7) the radial Regge trajectories are of the form

$$M^2 = \beta_{n_r}\left(n_r + c_0'\right)^{2/3} + c_1', \tag{15}$$

and the orbital Regge trajectories take the form

$$M^2 = \beta_l\left(l + c_0''\right)^{2/3} + c_1''. \tag{16}$$

By considering Eqs. (15) and (16), we find that the Regge trajectories for mesons composed of different quarks can be rewritten in the same form as the Regge trajectories for heavy quarkonia [25], see Eq. (1).

In Ref. [25], we have shown that the new form of the Regge trajectories [Eq. (1)] are appropriate to the heavy quarkonia. In this work, we show that Eq. (1) can also be appropriate to

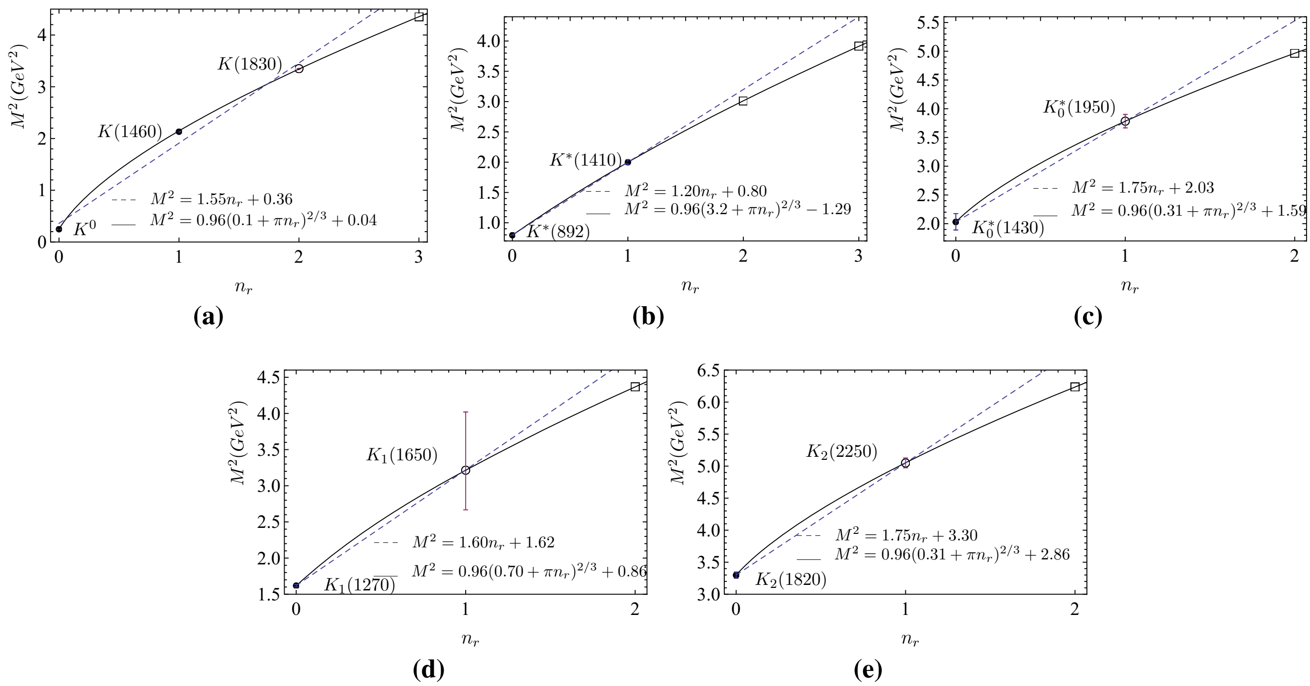

Fig. 1 The radial Regge trajectories for the strange mesons. The used data are listed in Table 1. The well-established states are given by the solid dots. The unwell-established states or the states needing confirmation are given by circles. Open squares are predicted masses by the fitted Regge trajectories. The dashed lines are the fitted linear Regge trajectories and the solid lines are the fitted curves by using Eq. (1)

the mesons consisting of different quarks. The new form of the Regge trajectories is expected to be universal for mesons. The good fit by employing Eq. (1) illustrates this conclusion.

3 Regge trajectories for the mesons constituting of different quarks

In this section, we employ the Regge trajectory formula $M^2 = \beta\,(c_l l + \pi n_r + c_0)^{2/3} + c_1$ [Eq. (1)] to fit the spectra of the strange mesons, the heavy-light mesons and the bottom-charmed mesons. The parameters of the Regge trajectories are obtained by fitting the experimental data or theoretical values. The fitted radial and orbital Regge trajectories are in agreement with the experimental data or the theoretical predictions. The linear Regge trajectories are also given and we find that the new form of the Regge trajectories are better than the linear ones.

3.1 Strange mesons

The universal parameter β is calculated by fitting the radial Regge trajectories for K^0 and $K^*(892)$, $\beta = 0.96$ for the strange mesons. The universal parameter c_l is obtained by fitting the orbital Regge trajectories for $K^*(892)$, $c_l = 4.47$. c_0 and c_1 vary with different Regge trajectories. The fitted radial and orbital Regge trajectories are shown in Figs. 1 and 2. The fitted and predicted masses of the strange mesons by the Regge trajectories are listed in Table 1 and they are in good agreement with the experimental data and the theoretical values.

$K(1830)$ is suggested to be the 3^1S_0 state [41,43,44]. $K_0^*(1950)$ is taken as the 2^3P_0 state [41] and $K_2(2250)$ as a $2D_2$ state [17,41]. The mass of $K_1(1650)$ is $1793 \pm 59^{+153}_{-101}$ MeV [42] and $K_1(1650)$ is in favor of a $2P$ state [41]. In Refs. [41,43], $K_2^*(1980)$ is assumed to be the 2^3P_2 state or the 1^3F_2 sate [28]. As $K_2^*(1980)$ is treated as 1^3F_2 sate, the dominant decay channel is shown to be $K_1(1270)\pi$ which is not observed in experiments. $K_4(2500)$ is the possible candidate of the $2G$ state [17,41] and the fitted value is in accordance with the experimental data. $K_5^*(2380)$ is assigned as the 1^3G_5 state and needs confirmation [39]. Its mass is larger than the fitted value.

3.2 Charmed mesons

By fitting the radial Regge trajectories for D^0 and $D^*(2007)^0$, the universal parameter β is calculated, $\beta = 1.89$ for the charmed mesons. c_l is obtained by fitting the orbital Regge trajectories for D^0, $D^*(2007)^0$ and $D_0^*(2400)^0$, $c_l = 3.02$. c_0 and c_1 vary with different Regge trajectories. In Fig. 3 are the fitted radial and orbital Regge trajectories for the charmed mesons. The fitted and predicted masses of the charmed mesons by the Regge trajectories are listed in Table 2 and

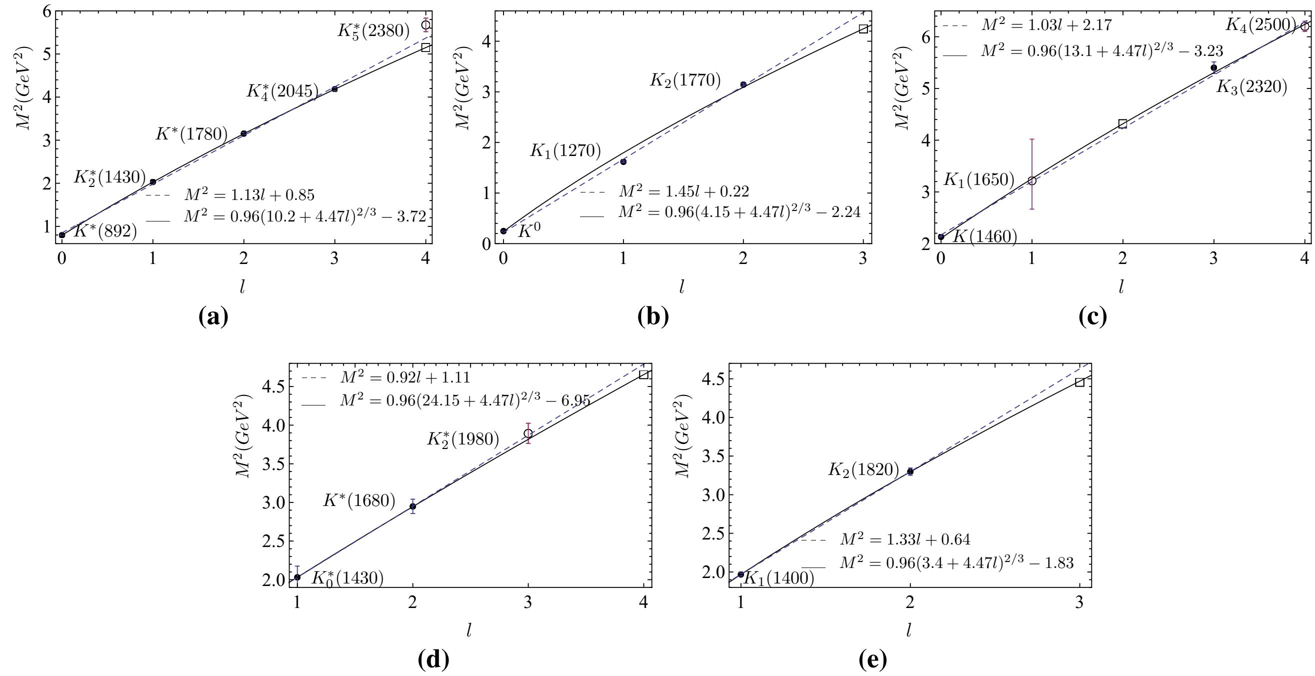

Fig. 2 Same as Fig. 1 except for the orbital Regge trajectories

Table 1 Masses of the strange mesons (in MeV). The experimental data are from PDG [39]. The fitted results by using the Regge trajectories [Eq. (1)] are shown in comparison with the theoretical values of GI [40], EFG [17] and PWLM [41]. ? denotes the possible candidates for the unwell-established states or the mesons needing confirmation. FO and FR denote the fitted results by the orbital Regge trajectories and by the radial Regge trajectories, respectively

State	J^P	Meson	PDG [39]	GI [40]	EFG [17]	PWLM [41]	FR	FO
1^1S_0	0^-	K^0	497.611 ± 0.013	461.5	482	497.7	497	489
2^1S_0	0^-	$K(1460)$	1460	1454	1538	1457	1464	1451
3^1S_0	0^-	$K(1830)$?	1830	2065	2065	1924	1829	
4^1S_0	0^-					2248	2087	
1^3S_1	1^-	$K^*(892)$	891.66 ± 0.26	902.8	897	896	891	892
2^3S_1	1^-	$K^*(1410)$	1414 ± 15	1579	1675	1548	1414	
3^3S_1	1^-			2156	2156	1983	1735	
4^3S_1	1^-					2287	1979	
1^3P_0	0^+	$K_0^*(1430)$	1425 ± 50	1234	1362	1257	1425	1426
2^3P_0	0^+	$K_0^*(1950)$?	$1945 \pm 10 \pm 20$	1890	1791	1829	1945	
3^3P_0	0^+			2160	2160	2176	2228	
1^1P_1	1^+	$K_1(1270)$	1272 ± 7	1352	1294	1364	1272	1340
2^1P_1	1^+	$K_1(1650)$?	$1793 \pm 59^{+153}_{-101}$ [42]	1897	1757	1840	1793	1805
3^1P_1	1^+			2164	2164	2177	2090	
1^3P_1	1^+	$K_1(1400)$	1403±7	1366	1412	1377		1403
1^3P_2	2^+	$K_2^*(1430)$	1425.6 ± 1.5	1428	1424	1431		1426
1^3D_1	1^-	$K^*(1680)$	1717 ± 27	1776	1699	1766		1716
1^1D_2	2^-	$K_2(1770)$	1773±8	1791	1709	1778		1758
2^1D_2	2^-			2238	2066	2121		2078
1^3D_2	2^-	$K_2(1820)$	1816±13	1804	1824	1789	1817	1816
2^3D_2	2^-	$K_2(2250)$?	2247±17	2254	2163	2131	2248	
3^3D_2	2^-					2388	2497	

Table 1 continued

State	J^P	Meson	PDG [39]	GI [40]	EFG [17]	PWLM [41]	FR	FO
1^3D_3	3^-	$K_3^*(1780)$	1776 ± 7	1794	1789	1781		1775
1^3F_2	2^+	$K_2^*(1980)$?	$1973 \pm 8 \pm 25$	2151	1964	2093		1954
1^1F_3	3^+			2131	2009	2075		2060
2^1F_3	3^+	$K_3(2320)$	2324 ± 24	2524	2348	2340		2303
1^3F_3	3^+			2143	2080	2084		2114
1^3F_4	4^+	$K_4^*(2045)$	2045 ± 9	2108	2096	2058		2045
1^1G_4	4^-			2422	2255	2309		2303
2^1G_4	4^-	$K_4(2500)$?	2490 ± 20	2779	2575	2520		2498
1^3G_4	4^-			2433	2285	2317		2354
1^3G_5	5^-	$K_5^*(2380)$?	$2382 \pm 14 \pm 19$	2388	2356	2286		2269

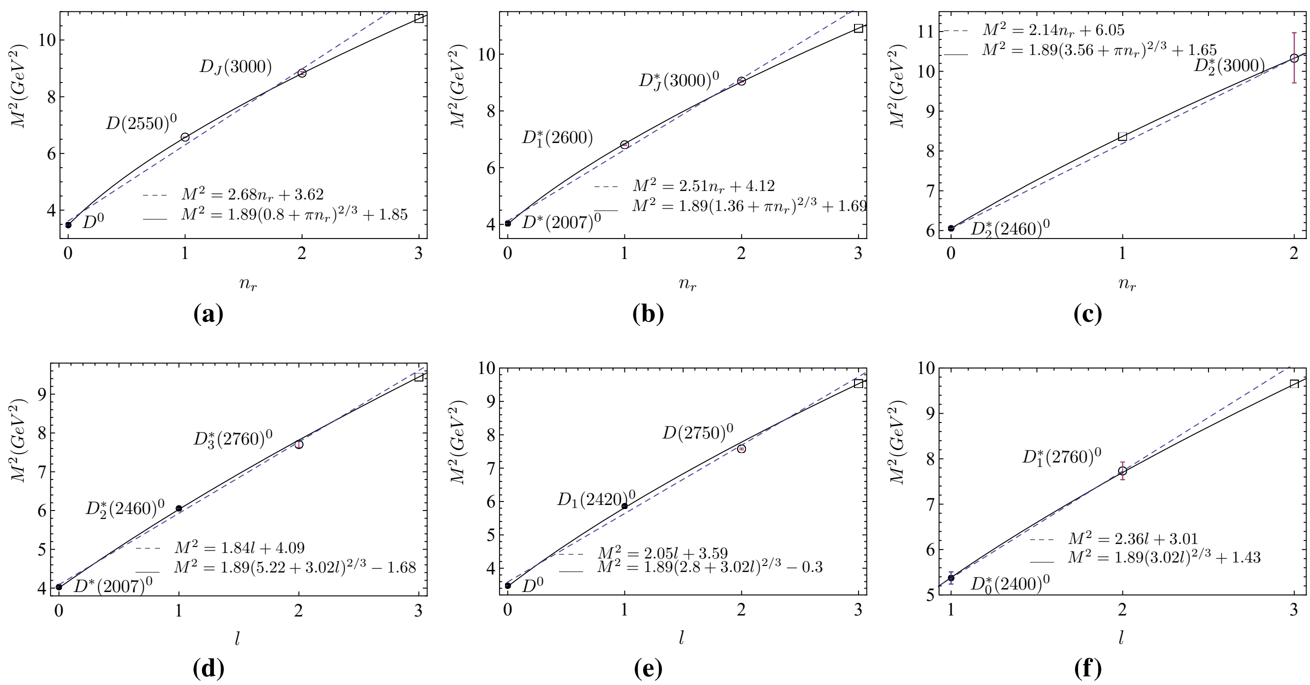

Fig. 3 The radial and orbital Regge trajectories for the charmed mesons. The used data are listed in Table 2. The well-established states are given by solid dots. The unwell-established states or the states needing confirmation are given by circles. Open squares are predicted masses by the fitted Regge trajectories

they are consistent with the experimental data and the theoretical values.

$D(2550)$ is taken as a candidate for the 2^1S_0 state by the helicity distribution analysis [45], and $D_J(2580)$ is assumed to be the same state because the resonance parameters of $D_J(2580)$ and $D(2550)$ are similar and BaBar assignment [45] is consistent with the LHCb results [46]. $D_J(3000)$ is a possible candidate for the $2P$ state [47], the 3^1S_0 state [48], or the 3^+ state [49]. $D^*(2600)$ can be assigned to be the 2^3S_1 state [48,50], see Ref. [51] for more discussions. $D_J^*(3000)^0$ can be the candidate of the 3^3S_1 state [51]. $D_2^*(3000)$ is possibly the 3^3P_2 state while the assignment of the 2^3F_2 state can not be fully excluded [52]. $D(2750)^0$ is assigned as the $1D_2$ state [53,54]. $D_1^*(2760)$ and $D_3^*(2760)$ are assumed to be the 1^3D_1 state and 1^3D_3 state [53,55–59], respectively.

3.3 Charmed-strange mesons

Due to insufficient experimental data, the radial Regge trajectory for the charmed-strange mesons are obtained by fitting the theoretical values in Ref. [60], $\beta = 1.75$, see Fig. 4a. The orbital Regge trajectories by fitting the experimental data and by fitting the theoretical values in Ref. [60] are in consistence, see Fig. 4b. The universal parameter is calculated, $c_l = 2.44$. The experimental data and the theoretical predictions are listed in Table 3.

Table 2 Masses of the charmed mesons (in MeV). The experimental data are from PDG [39]. The theoretical values are from EFG [16], GM [53], KDR [54] and LNR [60]. ? denotes the possible candidates for the unwell-established states or the mesons needing confirmation. FO and FR denote the fitted results by the orbital Regge trajectories and by the radial Regge trajectories, respectively

State	J^P	Meson	PDG [39]	EFG [16]	GM [53]	KDR [54]	LNR [60]	FR	FO
1^1S_0	0^-	D^0	1864.83 ± 0.05	1871	1877	1884	1874	1865	1859
		$D^\pm$	1869.58 ± 0.09						
2^1S_0	0^-	$D(2550)^0$?	2564 ± 20	2581	2581	2582	2540	2562	
		$D_J(2580)^0$?	$2579.5 \pm 3.4 \pm 5.5$ [46]						
3^1S_0	0^-	$D_J(3000)^0$?	2971.8 ± 8.7 [46]	3062	3068	3186	2904	2970	
4^1S_0	0^-			3452	3468	3746	3175	3279	
5^1S_0	0^-			3793	3814	4283		3535	
1^3S_1	1^-	$D^*(2007)^0$	2006.85 ± 0.05	2010	2041	2010	2006	2003	2002
		$D^*(2010)^\pm$	2010.26 ± 0.05						
2^3S_1	1^-	$D_1^*(2600)$?	$2608.7 \pm 2.4 \pm 2.5$ [45]	2632	2643	2655	2601	2616	
3^3S_1	1^-	$D_J^*(3000)^0$?	3008.1 ± 4.0 [46]	3096	3110	3239	2947	3004	
4^3S_1	1^-			3482	3497	3789	3208	3304	
5^3S_1	1^-			3822	3837	4319		3554	
1^3P_0	0^+	$D_0^*(2400)^0$	2318 ± 29	2406	2399	2357	2341		2319
		$D_0^*(2400)^\pm$	2351 ± 7						
1^1P_1	1^+	$D_1(2420)^0$	2420.8 ± 0.5	2426	2456	2425	2389		2411
1^3P_1	1^+	$D_1(2430)^0$	$2427 \pm 26 \pm 25$	2469	2467	2447	2407		2427
		$D_1(2420)^\pm$	2423.2 ± 2.4						
1^3P_2	2^+	$D_2^*(2460)^0$	2460.57 ± 0.15	2460	2502	2461	2477	2461	2456
		$D_2^*(2460)^\pm$	2465.4 ± 1.3						
2^3P_2	2^+			3012	2957	3039	2860	2893	
3^3P_2	2^+	$D_2^*(3000)$?	$3214 \pm 29 \pm 33 \pm 36$ [61]	3407	3353	3584	3142	3214	
1^3D_1	1^-	$D_1^*(2760)$?	$2781 \pm 18 \pm 11 \pm 6$ [55,56]	2788	2817	2755	2750		2775
1^1D_2	2^-	$D(2750)^0$?	$2752.4 \pm 1.7 \pm 2.7$ [45]	2806	2816	2754	2689		2789
1^3D_2	2^-	$D(2740)^0$?	$2737.0 \pm 3.5 \pm 11.2$	2850	2845	2783	2727		2737
1^3D_3	3^-	$D_3^*(2760)^0$?	$2775.5 \pm 4.5 \pm 4.5 \pm 4.7$ [61]	2863	2833	2788	2688		2796
1^3F_2	2^+			3090	3132				3105
1^1F_3	3^+			3129	3108				3087
1^3F_3	3^+			3145	3143				2998
1^3F_4	4^+			3187	3113				3073

$D_{s1}^*(2700)^\pm$ is assigned as the 2^3S_1 state [40,62–64]. $D_{s1}^*(2700)^\pm$ is taken as the 2^1S_0 state in Ref. [65] or is suggested to be a mixture of the 2^3S_1 and 1^3D_1 states [66–68]. In Refs. [57,69–71], $D_{s1}^*(2860)$ and $D_{s3}^*(2860)$ are taken as the 1^3D_1 state and the 1^3D_3 state, respectively. In Ref. [72], $D_{s1}^*(2860)$ is interpreted as a mixture of $D_s(2^3S_1)$ and $D_s(1^3D_1)$.

3.4 $B/B_s/B_c$

For the bottom mesons, the bottom-strange meson, especially for the bottom-charmed mesons, the experimental data are scarce and the theoretical values are used to fit the radial and orbital Regge trajectories.

For the bottom mesons, the theoretical values in [60] are used. The fitted universal parameters are $\beta = 2.69$ and $c_l = 1.74$. The Regge trajectories are shown in Fig. 5, and the experimental and theoretical values are listed in Table 4.

$B_J(5840)^0$ is suggested to be the 2^1S_0 state [73,74]. The $B_J(5960)^0$ and $B(5970)^0$ are probably the same state. In [74], $B(5970)^0/B_J(5960)^0$ is interpreted as 2^3S_1 or 1^3D_3 states [75]. In Refs. [76,77], $B(5970)^0$ is takes as the 2^3S_1 state. In Ref. [78], $B(5970)^0$ is assumed to be the 2^3S_1, 1^3D_1 and 1^3D_3 states.

For the bottom-strange mesons, $\beta = 1.75$ and $c_l = 2.44$. The radial and orbital Regge trajectories are given by fitting the theoretical predictions in Ref. [60], see Fig. 6. The experimental and theoretical data are in Table 5.

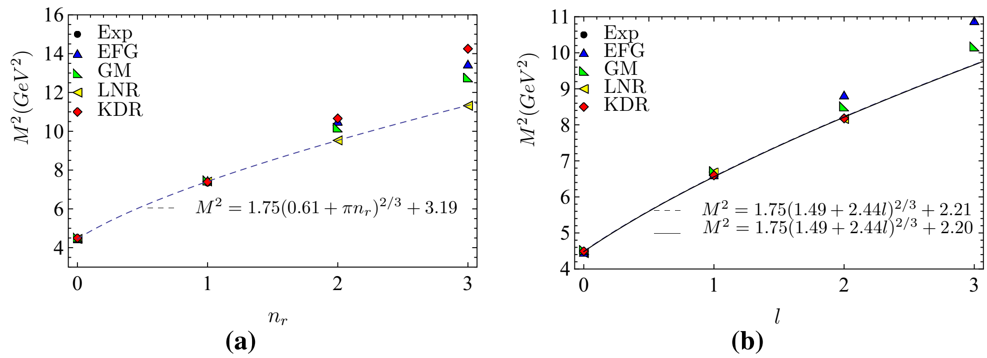

Fig. 4 (Color online) The radial and orbital Regge trajectories for the charmed-strange mesons. The theoretical data are from Ref. [16] (EFG), [53] (GM), [54] (KDR) and [60] (LNR). The experimental data (Exp) are from Ref. [39]. The dashed lines are the fitted Regge trajectories for the theoretical values in [60] while the solid line is for the experimental data from [39]

Table 3 Masses of the charmed-strange mesons (in MeV). The experimental data are from PDG [39]. The theoretical values are from EFG [16], GM [53], KDR [54] and LNR [60]. ? denotes the possible candidates for the unwell-established states or the mesons needing confirmation

State	J^P	Meson	PDG [39]	EFG [16]	GM [53]	KDR [54]	LNR [60]
1^1S_0	0^-	$D_s^{\pm}$	1968.27 ± 0.10	1969	1979	1965	1975
1^3S_1	1^-	$D_s^{*\pm}$	2112.1 ± 0.4	2111	2129	2120	2108
2^3S_1	1^-	$D_{s1}^*(2700)^{\pm}$?	$2708.3^{+4.0}_{-3.4}$	2731	2732	2719	2722
3^3S_1	1^-			3242	3193	3265	3087
4^3S_1	1^-			3669	3575	3775	3364
1^3P_0	0^+	$D_{s0}^*(2317)^{\pm}$	2317.7 ± 0.6	2509	2484	2438	2455
1^1P_1	1^+	$D_{s1}(2536)^{\pm}$	2535.10 ± 0.06	2536	2549	2529	2502
1^3P_1	1^+	$D_{s1}(2460)^{\pm}$	2459.5 ± 0.6	2574	2556	2541	2522
1^3P_2	2^+	$D_{s2}^*(2573)$	2569.1 ± 0.8	2571	2592	2569	2586
1^3D_1	1^-	$D_{s1}^*(2860)^{\pm}$?	$2859 \pm 12 \pm 24$	2913	2899	2882	2845
1^1D_2	2^-			2931	2900	2853	2838
1^3D_3	3^-	$D_{s3}^*(2860)^{\pm}$?	$2860.5 \pm 2.6 \pm 6.5$	2971	2917	2860	2857
1^3F_2	2^+			3230	3208		
1^1F_3	3^+			3254	3186		
1^3F_4	4^+			3300	3190		

By fitting the theoretical values in Ref. [79], we obtain the Regge trajectories for the bottom-charmed mesons, $\beta = 3.49$ and $c_l = 1.75$, see Fig. 7. In Table 6 are the experimental and theoretical values.

Up to date, only two B_c states have been observed. B_c^+ is well established [80–84]. $B_c(2S)$ was observed by the ATLAS Collaboration [85] but has not been confirmed [86].

4 Discussions

In this section, two important properties, the universality and the concavity, of the Regge trajectories are discussed.

4.1 Universality of the new form of the Regge trajectories

In Ref. [25], we obtained one new form of the Regge trajectories [Eq. (1)] from the QSSE and showed that heavy quarkonia can be well described by Eq. (1) by fitting the spectra of charmonia and bottomonia. In the present work, the case of the mesons consisting of unequally massive quarks are considered and the obtained Regge trajectories have the same form as the Regge trajectories for heavy quarkonia. Then we apply the obtained Regge trajectories to fit the spectra of the strange mesons, the heavy-light mesons (the D, D_s, B and B_s mesons) and the B_c mesons. The fitted Regge trajectories are in agreement with the experimental data and the theoretical predictions. The new form of the Regge trajectories is expected to be appropriate also for the light unflavored

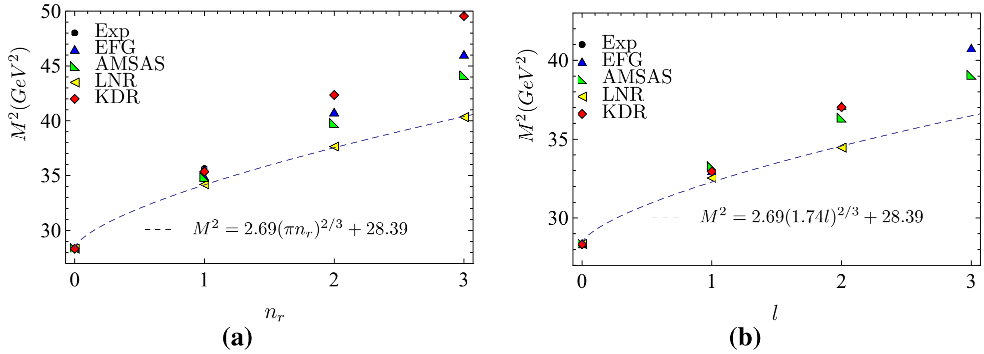

Fig. 5 (Color online) The radial and orbital Regge trajectories for the bottom mesons. The theoretical data are from Ref. [16] (EFG), [88] (AMSAS), [87] (KDR) and [60] (LNR). The experimental data (Exp) are from Ref. [39]. The dashed lines are the Regge trajectories by fitting the theoretical values in [60]

Table 4 Masses of the bottom mesons (in MeV). The experimental data are from PDG [39]. The theoretical values are from EFG [16],KDR [87], LNR [60] and AMSAS [88]. ? denotes the possible candidates for the unwell-established states or the mesons needing confirmation

State	J^P	Meson	PDG [39]	EFG [16]	KDR [87]	LNR [60]	AMSAS [88]
1^1S_0	0^-	B^0	5279.62 ± 0.15	5280	5287	5277	5268
2^1S_0	0^-	$B_J(5840)^0$?	5863 ± 9	5890	5926	5822	5877
3^1S_0	0^-			6379	6492	6117	6288
4^1S_0	0^-			6781	7027	6335	6631
1^3S_1	1^-	B^*	5324.65 ± 0.25	5326	5323	5325	5329
2^3S_1	1^-	$B_J(5960)^0$?	$5969.2 \pm 2.9 \pm 5.1 \pm 0.2$ [73]	5906	5947	5848	5905
3^3S_1	1^-			6387	6508	6136	6308
4^3S_1	1^-			6786	7039	6351	6647
1^1P_1	1^+	$B_1(5721)^0$	5726.0 ± 1.3	5723	5733	5686	5755
1^3P_2	2^+	$B_2^*(5747)^0$	5739.5 ± 0.7	5741	5740	5704	5769
1^3D_3	3^-			6091	6085	5871	6031
1^3F_4	4^+			6385			6252

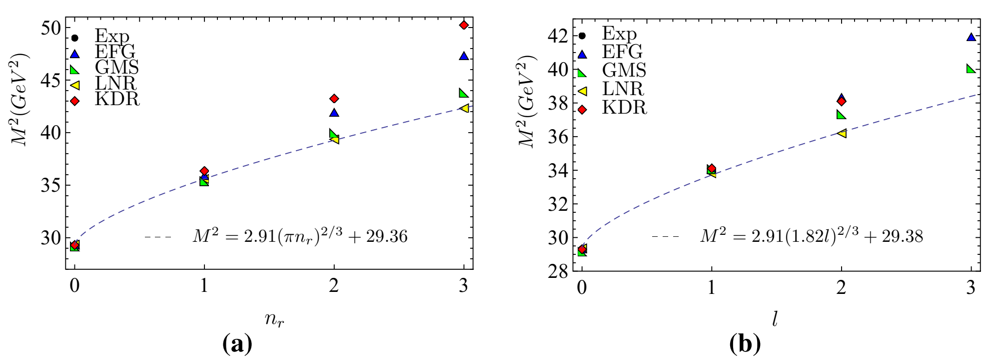

Fig. 6 (Color online) The radial and orbital Regge trajectories for the bottom-strange mesons. The theoretical data are from Ref. [16] (EFG), [89] (GMS), [87] (KDR) and [60] (LNR). The experimental data (Exp) are from Ref. [39]. The dashed lines are the Regge trajectories by fitting the theoretical values in [60]

mesons, for example, see Fig. 8. Therefore, we conclude that the new form the Regge trajectories [Eq. (1)] can be appropriate not only for the heavy mesons but also for the light mesons, not only for the mesons composed of the same quarks but also for the mesons composed of different quarks, that is to say, Eq. (1) is expected to be universal for mesons.

The parameters β_{n_r} of the radial Regge trajectories and β_l of the orbital Regge trajectories are listed in Tables 7 and 8, respectively. For mesons except for the light mesons, β_{n_r}

Table 5 Masses of the bottom mesons (in MeV). The experimental data are from PDG [39]. The theoretical values are from EFG [16], GMS [89], LNR [60] and KDR [87]. ? denotes the possible candidates for the unwell-established states or the mesons needing confirmation

State	J^P	Meson	PDG [39]	EFG [16]	GMS [89]	LNR [60]	KDR [87]
1^1S_0	0^-	B_s^0	5366.82 ± 0.22	5372	5366	5366	5367
1^3S_1	1^-	B_s^*	$5415.4^{+1.8}_{-1.5}$	5414	5400	5417	5413
2^3S_1	1^-			5992	5948	5966	6029
3^3S_1	1^-			6475	6319	6274	6575
4^3S_1	1^-			6879	6617	6504	7087
1^1P_1	1^+	$B_{s1}(5830)^0$	5828.63 ± 0.27	5831	5830	5795	5842
1^3P_2	2^+	$B_{s2}^*(5840)^0$	5839.84 ± 0.18	5842	5836	5815	5840
1^3D_3	3^-			6191	6109	6016	6172
1^3F_4	4^+			6475	6328		

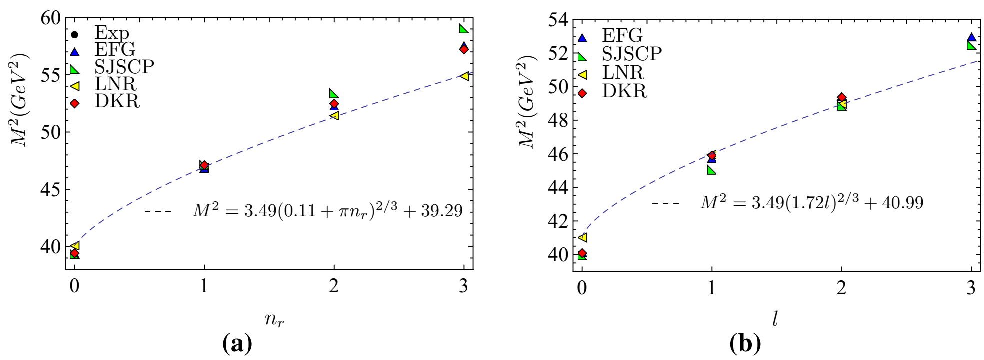

Fig. 7 (Color online) The radial and orbital Regge trajectories for the bottom-charmed mesons. The theoretical data are from Ref. [90] (EFG), [91] (SJSCP), [92] (DKR) and [79] (LNR). The experimental data (Exp) are from Ref. [39]. The dashed lines are the Regge trajectories by fitting the theoretical values in [79]

Table 6 Masses of the bottom mesons (in MeV). The experimental data are from PDG [39]. The theoretical values are from EFG [16],KDR [87], LNR [60] and AMSAS [88]. ? denotes the possible candidates for the unwell-established states or the mesons needing confirmation

State	J^P	Meson	PDG [39]	EFG [90]	SJSCP [91]	DKR [92]	LNR [79]
1^1S_0	0^-	B_c^+	6275.1 ± 1.0	6272	6272	6278	6330
2^1S_0	0^-	$B_c(2S)^{\pm}$?	$6842 \pm 4 \pm 5$	6842	6864	6863	6850
3^1S_0	0^-			7226	7306	7244	7171
4^1S_0	0^-			7585	7684	7564	7408
1^3S_1	1^-			6333	6321	6331	6404
1^3P_2	2^+			6761	6712	6775	6779
1^3D_3	3^-			7029	6990	7026	6998
1^3F_4	4^+			7277	7244		

and β_l increase with the quark mass, and there is the relation $\beta_{n_r} > \beta_l$. The exception of the light mesons maybe arises from the complexity of the light mesons.

4.2 Concavity of the Regge trajectories

In Refs. [23,90,93–98], the fitted curves showed evidently the concavity of the Regge trajectories although the authors did not point out explicitly the curvature of the meson Regge trajectories. In Refs. [14,99,100], the authors noticed the curvature of the Regge trajectories for mesons but a few Regge trajectories were fitted, therefore, the generality of the concavity can not be illustrated.

In Ref. [25], we have shown that the bottomonia and charmonia can be well described by the concave formula (1). In Sect. 3, the strange mesons, the heavy-light mesons (the

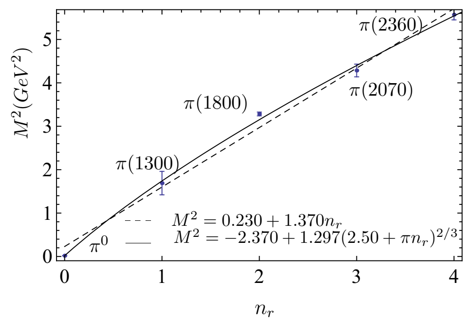

Fig. 8 The radial Regge trajectories for π [25]

Table 7 β_{n_r} of the radial Regge trajectories. $\beta_{n_r} = \beta\pi^{2/3}$. n represents the up quark or down quark

	$\bar{n}$	$\bar{s}$	$\bar{c}$	$\bar{b}$
n	2.78[a]	2.06	4.05	5.77[c]
s	2.06	–[b]	3.75[c]	6.24[c]
c	4.05	3.75[c]	4.33	7.49[c]
b	5.77[c]	6.24[c]	7.49[c]	10.94

[a]The coefficient is from the radial Regge trajectory for π^0
[b]The radial Regge trajectories for $\eta'(958)$ and for $\phi(1020)$ seem convex which need confirmation. See Ref. [101] for more discussions
[c]These coefficients are from the radial Regge trajectories by fitting the theoretical values in Refs. [60,79]

Table 8 β_l of the orbital Regge trajectories. $\beta_l = \beta c_l^{2/3}$. n represents the up quark or down quark

	$\bar{n}$	$\bar{s}$	$\bar{c}$	$\bar{b}$
n	3.89[a]	2.61	3.95	3.89[c]
s	2.61	2.36[b]	3.17[c]	4.34[c]
c	3.95	3.17[c]	3.53	5.01[c]
b	3.89[c]	4.34[c]	5.01[c]	9.27

[a]The coefficient is from the orbital Regge trajectory for $\rho(770)$
[b]The coefficient is from the orbital Regge trajectory for $\phi(1020)$
[c]These coefficients are from the orbital Regge trajectories by fitting the theoretical values in Refs. [60,79]

D, D_s, B and B_s) and the bottom-charmed mesons are discussed by the formula (1). The Regge trajectories [Eq. (1)] are appropriate also for some light unflavored mesons, for example, see Fig. 8. The Regge trajectories will be concave if the spectra can be described by a concave formula, therefore, the concavity of the Regge trajectories for these mesons is independent of the models which the employed formula comes from. See Ref. [101] for more discussions.

It is one of the fundamental properties whether the meson Regge trajectories are linear, concave, convex or have the inflection points. For the potential models, the concavity of the Regge trajectories is of cardinal significance because it is related to the choice of the appropriate dynamic equation or the appropriate potential. If the confining potential is linear [102–116], the Schrödinger equation produces the convex Regge trajectories while the spinless Salpeter equation [13,117], the Dirac equation [118] and the Klein–Gordon equation [119–123] give the linear Regge trajectories. The QSSE [25,31,101] and the eigenvalue equation for the square mass operator lead to the concave Regge trajectories. There exist other possibilities. For example, if the confining potential takes the form $r^{0.1}$ [124,125] or $r^{1/2}$ [126–128], all dynamic equations mentioned above can yield the concave Regge trajectories. In this case, more information is needed to choose the appropriate dynamic equation and the corresponding confinement potential.

5 Conclusions

In this paper, we obtain the radial and orbital Regge trajectories for the mesons composed of unequally massive quarks from the QSSE by employing the Bohr–Sommerfeld quantization approach. The obtained Regge trajectories have the same form as the Regge trajectories for heavy quarkonia [25], $M^2 = \beta\,(c_l l + \pi n_r + c_0)^{2/3} + c_1$. By fitting the spectra of the strange mesons, the heavy-light mesons (the D, D_s, B and B_s mesons) and the bottom-charmed mesons, we show that the fitted Regge trajectories are in agreement with the experimental data and the theoretical predictions. By combining the results in Ref. [25] and in the present work, we expect that the new form of the Regge trajectories will be universal for mesons.

By fitting the spectra of mesons, the concavity of these Regge trajectories is illustrated. This property is of cardinal significance for the potential models because it can assist in the choice of the appropriate dynamic equation or the appropriate potential to describe mesons. If the confinement potential is linear, the Schrödinger equation arouses the convex Regge trajectories while the Dirac equation, the Klein–Gordon equation and the spinless Salpeter equation will produce the linear Regge trajectories. The QSSE [Eq. (4)] and the eigenvalue equation for the square mass operator [Eq. (2)] can give the concave Regge trajectories. Therefore, the QSSE and the eigenvalue equation for the square mass operator are preferred if the confinement potential is linear. If the confinement potential takes the form $r^{0.1}$ or $r^{1/2}$, all the dynamic equations mentioned above can yield the concave Regge trajectories. In this case, more information is needed to choose the appropriate dynamic equation and the corresponding potential.

Funded by SCOAP^3.

References

1. T. Regge, Nuovo Cim. **14**, 951 (1959)
2. G.F. Chew, S.C. Frautschi, Phys. Rev. Lett. **7**, 394 (1961)
3. G.F. Chew, S.C. Frautschi, Phys. Rev. Lett. **8**, 41 (1962)
4. Y. Nambu, Phys. Rev. D **10**, 4262 (1974)
5. Y. Nambu, Phys. Lett. B **80**, 372 (1979)
6. M. Ademollo, G. Veneziano, S. Weinberg, Phys. Rev. Lett. **22**, 83 (1969)
7. M. Baker, R. Steinke, Phys. Rev. D **65**, 094042 (2002). arXiv:hep-th/0201169
8. J. Polchinski, M.J. Strassler, Phys. Rev. Lett. **88**, 031601 (2002). arXiv:hep-th/0109174
9. A. Karch, E. Katz, D.T. Son, M.A. Stephanov, Phys. Rev. D **74**, 015005 (2006). arXiv:hep-ph/0602229
10. S.J. Brodsky, Eur. Phys. J. A **31**, 638 (2007). arXiv:hep-ph/0610115
11. H. Forkel, M. Beyer, T. Frederico, JHEP **0707**, 077 (2007). arXiv:0705.1857 [hep-ph]
12. S. Filipponi, Y. Srivastava, Phys. Rev. D **58**, 016003 (1998). arXiv:hep-ph/9712204
13. F. Brau, Phys. Rev. D **62**, 014005 (2000). arXiv:hep-ph/0412170
14. M.M. Brisudova, L. Burakovsky, T. Goldman, Phys. Rev. D **61**, 054013 (2000). arXiv:hep-ph/9906293
15. X.H. Guo, K.W. Wei, X.H. Wu, Phys. Rev. D **78**, 056005 (2008). arXiv:0809.1702 [hep-ph]
16. D. Ebert, R.N. Faustov, V.O. Galkin, Eur. Phys. J. C **66**, 197 (2010). arXiv:0910.5612 [hep-ph]
17. D. Ebert, R.N. Faustov, V.O. Galkin, Phys. Rev. D **79**, 114029 (2009). arXiv:0903.5183 [hep-ph]
18. W. Buchmuller, G. Grunberg, S.H.H. Tye, Phys. Rev. Lett. **45**, 103 (1980) [Erratum: Phys. Rev. Lett. **45**, 587 (1980)]
19. J.L. Gervais, A. Neveu, Nucl. Phys. B **163**, 189 (1980)
20. C. Lovelace, Phys. Lett. **28B**, 264 (1968)
21. A.C. Irving, R.P. Worden, Phys. Rep. **34**, 117 (1977)
22. P.D.B. Collins, Phys. Rep. **1**, 103 (1971)
23. G.S. Sharov, arXiv:hep-ph/1305.3985
24. K. Chen, Y.B. Dong, X. Liu, Q.F. Lü, T. Matsuki, Eur. Phys. J. C **78**(1), 20 (2018). arXiv:1709.07196 [hep-ph]
25. J.K. Chen, Eur. Phys. J. C **78**(3), 235 (2018)
26. M. Baldicchi, Conference: C99-09-29, 325 (2001). arXiv:hep-ph/9911268
27. N. Brambilla, E. Montaldi, G.M. Prosperi, Phys. Rev. D **54**, 3506 (1996). arXiv:hep-ph/9504229
28. M. Baldicchi, A.V. Nesterenko, G.M. Prosperi, C. Simolo, Phys. Rev. D **77**, 034013 (2008). arXiv:0705.1695 [hep-ph]
29. M. Baldicchi, A.V. Nesterenko, G.M. Prosperi, D.V. Shirkov, C. Simolo, Phys. Rev. Lett. **99**, 242001 (2007). arXiv:0705.0329 [hep-ph]
30. M. Baldicchi, G.M. Prosperi, Phys. Rev. D **62**, 114024 (2000). arXiv:hep-ph/0008017
31. E. Di Salvo, L. Kondratyuk, P. Saracco, Z. Phys. C **69**, 149 (1995). arXiv:hep-ph/9411309
32. J.K. Chen, Acta Phys. Pol. B **47**, 1155 (2016)
33. J.K. Chen, Rom. J. Phys. **62**, 119 (2017)
34. S. Tomonaga, *Quantum Mechanics, Volume I: Old Quantum Theory* (North-Holland Publishing Company, Amsterdam, 1962)
35. E.E. Salpeter, H.A. Bethe, Phys. Rev. **84**, 1232 (1951)
36. E.E. Salpeter, Phys. Rev. **87**, 328 (1952)
37. E. Eichten, K. Gottfried, T. Kinoshita, J.B. Kogut, K.D. Lane, T.M. Yan, Phys. Rev. Lett. **34**, 369 (1975) [Erratum: Phys. Rev. Lett. **36**, 1276 (1976)]
38. I.S. Gradshteyn, I.M. Ryzhik, *Table of Integrals, Series, and Products*, corrected and enlarged edn. (Academic Press, New York, 1980)
39. C. Patrignani et al. (Particle Data Group), Chin. Phys. C **40**(10), 100001 (2016)
40. S. Godfrey, N. Isgur, Phys. Rev. D **32**, 189 (1985)
41. C.Q. Pang, J.Z. Wang, X. Liu, T. Matsuki, Eur. Phys. J. C **77**(12), 861 (2017). arXiv:1705.03144 [hep-ph]
42. R. Aaij et al. (LHCb Collaboration), Phys. Rev. Lett. **118**(2), 022003 (2017). arXiv:1606.07895 [hep-ex]
43. T. Barnes, N. Black, P.R. Page, Phys. Rev. D **68**, 054014 (2003). arXiv:nucl-th/0208072
44. J. Vijande, F. Fernandez, A. Valcarce, J. Phys. G **31**, 481 (2005). arXiv:hep-ph/0411299
45. P. del Amo Sanchez et al. (BaBar Collaboration), Phys. Rev. D **82**, 111101 (2010). arXiv:1009.2076 [hep-ex]
46. R. Aaij et al. (LHCb Collaboration), JHEP **1309**, 145 (2013). arXiv:1307.4556 [hep-ex]
47. Y. Sun, X. Liu, T. Matsuki, Phys. Rev. D **88**(9), 094020 (2013). arXiv:1309.2203 [hep-ph]
48. Q.F. Lü, D.M. Li, Phys. Rev. D **90**(5), 054024 (2014). arXiv:1407.3092 [hep-ph]
49. G.L. Yu, Z.G. Wang, Z.Y. Li, G.Q. Meng, Chin. Phys. C **39**(6), 063101 (2015). arXiv:1402.5955 [hep-ph]
50. Z.G. Wang, Phys. Rev. D **83**, 014009 (2011). arXiv:1009.3605 [hep-ph]
51. H.X. Chen, W. Chen, X. Liu, Y.R. Liu, S.L. Zhu, Rep. Prog. Phys. **80**(7), 076201 (2017). arXiv:1609.08928 [hep-ph]
52. J.Z. Wang, D.Y. Chen, Q.T. Song, X. Liu, T. Matsuki, Phys. Rev. D **94**(9), 094044 (2016). arXiv:1608.04186 [hep-ph]
53. S. Godfrey, K. Moats, Phys. Rev. D **93**(3), 034035 (2016). arXiv:1510.08305 [hep-ph]
54. V. Kher, N. Devlani, A.K. Rai, Chin. Phys. C **41**(7), 073101 (2017). arXiv:1704.00439 [hep-ph]
55. R. Aaij et al. (LHCb Collaboration), Phys. Rev. D **91**(9), 092002 (2015)
56. R. Aaij et al. (LHCb Collaboration), Phys. Rev. D **93**(11), 119901(E) (2016). arXiv:1503.02995 [hep-ex]
57. J.B. Liu, C.D. Lü, Eur. Phys. J. C **77**(5), 312 (2017). arXiv:1605.05550 [hep-ph]
58. R. Aaij et al. (LHCb Collaboration), Phys. Rev. D **92**(3), 032002 (2015). arXiv:1505.01710 [hep-ex]
59. B. Chen, X. Liu, A. Zhang, Phys. Rev. D **92**(3), 034005 (2015). arXiv:1507.02339 [hep-ph]
60. T.A. Lahde, C.J. Nyfalt, D.O. Riska, Nucl. Phys. A **674**, 141 (2000). arXiv:hep-ph/9908485
61. R. Aaij et al. (LHCb Collaboration), Phys. Rev. D **94**(7), 072001 (2016). arXiv:1608.01289 [hep-ex]
62. B. Zhang, X. Liu, W.Z. Deng, S.L. Zhu, Eur. Phys. J. C **50**, 617 (2007). arXiv:hep-ph/0609013
63. J. Segovia, D.R. Entem, F. Fernandez, Phys. Rev. D **91**(9), 094020 (2015). arXiv:1502.03827 [hep-ph]
64. G.L. Wang, J.M. Zhang, Z.H. Wang, Phys. Lett. B **681**, 326 (2009). arXiv:1001.2035 [hep-ph]
65. P. Colangelo, F. De Fazio, S. Nicotri, M. Rizzi, Phys. Rev. D **77**, 014012 (2008). arXiv:0710.3068 [hep-ph]
66. F.E. Close, C.E. Thomas, O. Lakhina, E.S. Swanson, Phys. Lett. B **647**, 159 (2007). arXiv:hep-ph/0608139
67. D.M. Li, B. Ma, Phys. Rev. D **81**, 014021 (2010). arXiv:0911.2906 [hep-ph]
68. X.H. Zhong, Q. Zhao, Phys. Rev. D **81**, 014031 (2010). arXiv:0911.1856 [hep-ph]
69. Q.T. Song, D.Y. Chen, X. Liu, T. Matsuki, Eur. Phys. J. C **75**(1), 30 (2015). arXiv:1408.0471 [hep-ph]
70. S. Godfrey, K. Moats, Phys. Rev. D **90**(11), 117501 (2014). arXiv:1409.0874 [hep-ph]
71. Z.G. Wang, Eur. Phys. J. C **75**(1), 25 (2015). arXiv:1408.6465 [hep-ph]

72. Q.T. Song, D.Y. Chen, X. Liu, T. Matsuki, Phys. Rev. D **91**, 054031 (2015). arXiv:1501.03575 [hep-ph]
73. R. Aaij et al. (LHCb Collaboration), JHEP **1504**, 024 (2015). arXiv:1502.02638 [hep-ex]
74. Q.F. Lü, T.T. Pan, Y.Y. Wang, E. Wang, D.M. Li, Phys. Rev. D **94**(7), 074012 (2016). arXiv:1607.02812 [hep-ph]
75. L.Y. Xiao, X.H. Zhong, Phys. Rev. D **90**(7), 074029 (2014). arXiv:1407.7408 [hep-ph]
76. Y. Sun, Q.T. Song, D.Y. Chen, X. Liu, S.L. Zhu, Phys. Rev. D **89**(5), 054026 (2014). arXiv:1401.1595 [hep-ph]
77. H. Xu, X. Liu, T. Matsuki, Phys. Rev. D **89**(9), 097502 (2014). arXiv:1402.0384 [hep-ph]
78. Z.G. Wang, Eur. Phys. J. Plus **129**, 186 (2014). arXiv:1401.7580 [hep-ph]
79. T.A. Lahde, C.J. Nyfalt, D.O. Riska, Nucl. Phys. A **645**, 587 (1999). arXiv:hep-ph/9808438 [Erratum: Nucl. Phys. A **665**, 447 (2000)]
80. F. Abe et al. (CDF Collaboration), Phys. Rev. Lett. **81**, 2432 (1998). arXiv:hep-ex/9805034
81. A. Abulencia et al. (CDF Collaboration), Phys. Rev. Lett. **96**, 082002 (2006). arXiv:hep-ex/0505076
82. T. Aaltonen et al. (CDF Collaboration), Phys. Rev. Lett. **100**, 182002 (2008). arXiv:0712.1506 [hep-ex]
83. V.M. Abazov et al. (D0 Collaboration), Phys. Rev. Lett. **101**, 012001 (2008). arXiv:0802.4258 [hep-ex]
84. R. Aaij et al. (LHCb Collaboration), Phys. Rev. Lett. **109**, 232001 (2012). arXiv:1209.5634 [hep-ex]
85. G. Aad et al. (ATLAS Collaboration), Phys. Rev. Lett. **113**(21), 212004 (2014). arXiv:1407.1032 [hep-ex]
86. R. Aaij et al. (LHCb Collaboration), JHEP **1801**, 138 (2018). arXiv:1712.04094 [hep-ex]
87. V. Kher, N. Devlani, A.K. Rai, Chin. Phys. C **41**(9), 093101 (2017). arXiv:1705.08248 [hep-ph]
88. I. Asghar, B. Masud, E.S. Swanson, F. Akram, M. Atif Sultan. Eur. Phys. J. A **54**(7), 127 (2018). arXiv:1804.08802 [hep-ph]
89. S. Godfrey, K. Moats, E.S. Swanson, Phys. Rev. D **94**(5), 054025 (2016). arXiv:1607.02169 [hep-ph]
90. D. Ebert, R.N. Faustov, V.O. Galkin, Eur. Phys. J. C **71**, 1825 (2011). arXiv:1111.0454 [hep-ph]
91. N.R. Soni, B.R. Joshi, R.P. Shah, H.R. Chauhan, J.N. Pandya, Eur. Phys. J. C **78**(7), 592 (2018). arXiv:1707.07144 [hep-ph]
92. N. Devlani, V. Kher, A.K. Rai, Eur. Phys. J. A **50**(10), 154 (2014)
93. J. Sonnenschein, D. Weissman, JHEP **1408**, 013 (2014). arXiv:1402.5603 [hep-ph]
94. S.S. Afonin, I.V. Pusenkov, Mod. Phys. Lett. A **29**(35), 1450193 (2014). arXiv:1308.6540 [hep-ph]
95. T. Branz, T. Gutsche, V.E. Lyubovitskij, I. Schmidt, A. Vega, Phys. Rev. D **82**, 074022 (2010). arXiv:1008.0268 [hep-ph]
96. K.W. Wei, X.H. Guo, Phys. Rev. D **81**, 076005 (2010)
97. S.S. Gershtein, A.K. Likhoded, A.V. Luchinsky, Phys. Rev. D **74**, 016002 (2006). arXiv:hep-ph/0602048
98. S.S. Afonin, I.V. Pusenkov, Phys. Rev. D **90**(9), 094020 (2014). arXiv:1411.2390 [hep-ph]
99. A. Inopin, G.S. Sharov, Phys. Rev. D **63**, 054023 (2001). arXiv:hep-ph/9905499
100. M.M. Brisudova, L. Burakovsky, J.T. Goldman, Phys. Lett. B **460**, 1 (1999). arXiv:hep-ph/9810296
101. J. K. Chen, arXiv:1807.11003 [hep-ph]
102. G.S. Bali, Phys. Rep. **343**, 1 (2001). arXiv:hep-ph/0001312
103. N. Brambilla et al. (Quarkonium Working Group), arXiv:hep-ph/0412158
104. T. Kawanai, S. Sasaki, Phys. Rev. D **85**, 091503 (2012). arXiv:1110.0888 [hep-lat]
105. J.B. Kogut, L. Susskind, Phys. Rev. D **9**, 3501 (1974)
106. K.G. Wilson, Phys. Rev. D **10**, 2445 (1974)
107. E.P. Tryon, Phys. Rev. Lett. **28**, 1605 (1972)
108. L.P. Fulcher, Phys. Rev. D **50**, 447 (1994)
109. C.R. Munz, J. Resag, B.C. Metsch, H.R. Petry, Nucl. Phys. A **578**, 418 (1994). arXiv:nucl-th/9307027
110. R. Ricken, M. Koll, D. Merten, B.C. Metsch, Eur. Phys. J. A **18**, 667 (2003). arXiv:hep-ph/0302124
111. D.P. Stanley, D. Robson, Phys. Rev. D **21**, 3180 (1980)
112. E. Eichten, K. Gottfried, T. Kinoshita, K.D. Lane, T.M. Yan, Phys. Rev. D **17**, 3090 (1978)
113. E. Eichten, K. Gottfried, T. Kinoshita, K.D. Lane, T.M. Yan, Phys. Rev. D **21**, 313(E) (1980)
114. E. Klempt, B.C. Metsch, C.R. Munz, H.R. Petry, Phys. Lett. B **361**, 160 (1995). arXiv:hep-ph/9507449
115. M.G. Olsson, S. Veseli, K. Williams, Phys. Rev. D **52**, 5141 (1995). arXiv:hep-ph/9503477
116. J.R. Spence, J.P. Vary, Phys. Rev. C **47**, 1282 (1993)
117. A. Martin, Z. Phys. C **32**, 359 (1986)
118. M.G. Olsson, S. Veseli, K. Williams, Phys. Rev. D **51**, 5079 (1995). arXiv:hep-ph/9410405
119. M.N. Sergeenko, Phys. At. Nucl. **56**, 365 (1993) [Yad. Fiz. **56N3**, 140 (1993)]
120. M.N. Sergeenko, Z. Phys. C **64**, 315 (1994)
121. J.S. Kang, H.J. Schnitzer, Phys. Rev. D **12**, 841 (1975)
122. L.K. Sharma, V.P. Iyer, J. Math. Phys. **23**, 1185 (1982)
123. C. Goebel, D. LaCourse, M.G. Olsson, Phys. Rev. D **41**, 2917 (1990)
124. A. Martin, Phys. Lett. **93B**, 338 (1980)
125. E.J. Eichten, C. Quigg, Phys. Rev. D **49**, 5845 (1994). arXiv:hep-ph/9402210
126. X.T. Song, H.F. Lin, Z. Phys. C **34**, 223 (1987)
127. L. Motyka, K. Zalewski, Z. Phys. C **69**, 343 (1996). arXiv:hep-ph/9503420
128. L. Motyka, K. Zalewski, Eur. Phys. J. C **4**, 107 (1998). arXiv:hep-ph/9709254